

controlled by computer.

For comparison of response latencies, freely walking flies were recorded using a Redlake Motionscope high-speed video recorder at 1,000 frames s⁻¹. Stimulus generation was as described above.

Localization and lateralization tasks

Stimulus duration was constant across all presentations, and the response of the fly did not modify the stimulus in any way (that is, the task was open loop). Unlike closed-loop stimulus conditions, in which the directional stimulus would decrease as the fly approached the angle of the speaker, here the angle of the speaker relative to the fly was fixed, and the fly received a constant turn signal throughout the stimulus. Therefore the fly's movements that generate the measured turn angles in these experiments could not bring them to face the direction of the speaker (turn angles should overshoot the actual speaker position). If the flies were simply lateralizing the stimulus source they would receive a constant turn signal (right or left) for the duration of the stimulus, and the angle of the flies' paths relative to the midline axis should be similar for all speaker positions. If the flies were truly localizing the sound source then paths for different speaker positions should be consistently different from one another and turn angle should increase with speaker angle.

Neurophysiology

Intracellular recordings were obtained from single auditory receptors using glass micro-electrodes (borosilicate, thin-walled 1.0 mm o.d., 70–120 MΩ). Receptors were recorded in the pterothoracic ganglion near the point of entry of the frontal nerve, which carries the auditory axons. After recordings, cells were injected with Lucifer Yellow and visualized under fluorescence microscopy to confirm that recordings were from primary receptors. Amplified (AM Systems Model 1600) neural responses were recorded by computer (100-kHz sampling rate) using an analogue-to-digital interface (TDT AD1). Stimuli were tone pulses of varying frequency and duration generated using the same system as in the behavioural experiments, but delivered through a different speaker (Realistic Horn Tweeter).

We obtained auditory nerve recordings using tungsten wire electrodes (AM Systems, 0.25 mm). Amplified (AM Systems Model 1800), summed action potentials from both nerves were recorded by computer (100-kHz sampling rate). We carried out recording and stimulation as described above. For these recordings, the preparation was mounted in the same apparatus that was used for the treadmill experiments, and responses from the two auditory nerves were recorded simultaneously for stimuli delivered from different angles of incidence. As the sampling rate of our acquisition system was limited to 100 kHz, the smallest angle of incidence measured in these experiments was 10°.

Received 4 September; accepted 20 December 2000.

1. Michelsen, A. in *The Evolutionary Biology of Hearing* (eds Webster, D. B., Fay, R. R. & Popper, A. N.) 61–78 (Springer, New York, 1992).
2. Robert, D., Amoroso, J. & Hoy, R. R. The evolutionary convergence of hearing in a parasitoid fly and its cricket host. *Science* **258**, 1135–1137 (1992).
3. Robert, D., Miles, R. N. & Hoy, R. R. Tympanal mechanics in the parasitoid fly *Ormia ochracea*: intertympanal coupling during mechanical vibration. *J. Comp. Physiol.* **183**, 443–452 (1998).
4. Miles, R. N., Robert, D. & Hoy, R. R. Mechanically coupled ears for directional hearing in the parasitoid fly *Ormia ochracea*. *J. Acoust. Soc. Am.* **98**, 3059–3070 (1995).
5. Robert, D., Read, M. P. & Hoy, R. R. Tympanal hearing in tachinid flies (Diptera, Tachinidae, Ormiini): The comparative morphology of an innovation. *Cell Tissue Res.* **284**, 435–448 (1996).
6. Gibbons, C. & Miles, R. N. in *Proceedings of the IMECE 5–20* (ASME, Orlando, Florida, 2000).
7. Fay, R. R. *Hearing in Vertebrates: A Psychophysics Databook* (Hill-Fay Associates, Winnetka, Illinois, 1988).
8. Rose, G. & Heiligenberg, W. Temporal hyperacuity in electric fish. *Nature* **318**, 178–180 (1985).
9. Kawasaki, M., Rose, G. & Heiligenberg, W. Temporal hyperacuity in single neurons of electric fish. *Nature* **336**, 173–176 (1988).
10. Walker, T. J. Phonotaxis in female *Ormia ochracea* (Diptera: Tachinidae), a parasitoid of field crickets. *J. Insect Behav.* **6**, 389–410 (1993).
11. Cade, W. H., Ciceran, M. & Murray, A. M. Temporal patterns of parasitoid fly (*Ormia ochracea*) attraction to field cricket song (*Gryllus integer*). *Can. J. Zool.* **74**, 393–395 (1996).
12. Ramsauer, N. *Phonotactic Behavior of Ormia ochracea (Diptera: Tachinidae, Ormiini) in Controlled Acoustic Conditions*. Thesis, Univ. Zurich (1999).
13. Robert, D. & Willi, U. The histological architecture of the auditory organs in the parasitoid fly *Ormia ochracea*. *Cell Tiss. Res.* **301**, 447–457 (2000).
14. Bair, W. & Koch, C. Temporal precision of spike trains in extrastriate cortex of the behaving macaque monkey. *Neural Comput.* **8**, 1185–1202 (1996).
15. Carr, C. E., Heiligenberg, W. & Rose, G. J. A time-comparison circuit in the electric fish midbrain. I. Behavior and physiology. *J. Neurosci.* **6**, 107–119 (1986).
16. Maršálek, P., Koch, C. & Maunsell, J. On the relationship between synaptic input and spike output jitter in individual neurons. *Proc. Natl Acad. Sci. USA* **94**, 735–740 (1997).
17. Rieke, F., Warland, D., de Ruyter van Steveninck, R. R. & Bialek, W. *Spikes* (MIT, Cambridge, Massachusetts, 1997).
18. Batschelet, E. *Circular Statistics in Biology* (Academic, New York, 1981).

Acknowledgements

We thank T. Adelman, D. Bodnar, B. Land, R. Wyttenbach, M. Andrade and all participants of NEJC. This work was supported by an NIH grant to R.R.H.

Correspondence and requests for materials should be addressed to A.C.M. (e-mail: amason@scar.utoronto.ca).

Motion direction, speed and orientation in binocular matching

Raymond van Ee*† & Barton L. Anderson*

*MIT Department of Brain and Cognitive Sciences, Cambridge, Massachusetts 02139, USA

†Utrecht University, Helmholtz Institute, Princeton Plein 5, 3584CC, Utrecht, The Netherlands

The spatial differences between the images seen by the two eyes, called binocular disparities, can be used to recover the volumetric (three-dimensional) aspects of a scene. The computation of disparity depends upon the correct identification of corresponding features in the two images. Understanding what image features are used by the brain to solve this matching problem is one of the main issues in stereoscopic vision¹. Many cortical neurons in visual areas V1 (ref. 2), MT (refs 3, 4) and MST (refs 5, 6) that are tuned to binocular disparity are also tuned to orientation, motion direction and speed. Although psychophysical work has shown that motion direction⁷ can facilitate binocular matching, the psychophysical literature on the role of orientation is mixed^{8,9}, and it has been argued that speed differences are ineffective in aiding correspondence⁷. Here we use a different psychophysical paradigm to show that the visual system uses similarities in orientation, motion direction and speed to achieve binocular correspondence. These results indicate that cells that multiplex orientation, motion direction, speed and

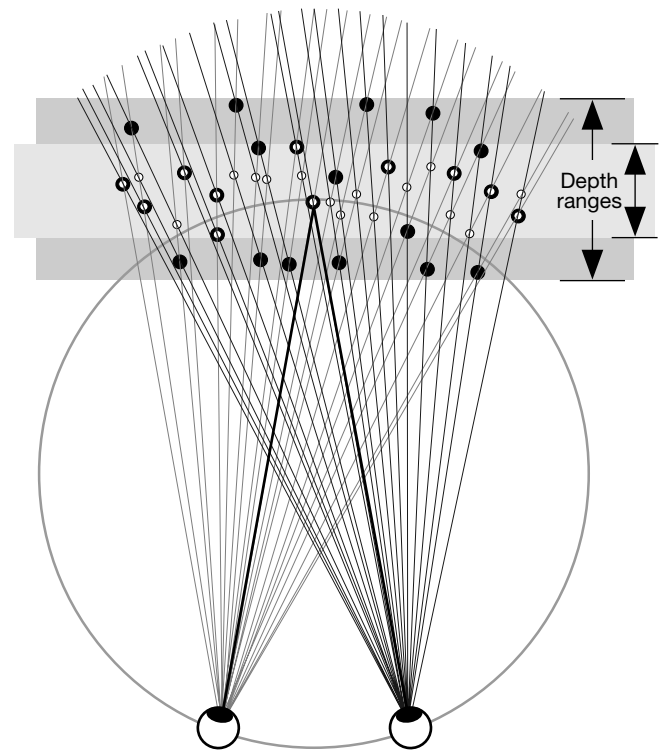


Figure 1 Top view of the geometry of the binocular matching problem. The intersections of the visual lines indicate the locations of possible matches. The drawing is schematic; contours in three dimensions introduce another dimension of ambiguity (namely, determining how correspondence between portions of the contours in the two eyes should be defined). One configuration represents a large depth range (black dots), the other a small depth range (white dots). The two configurations create identical sets of visual lines.

binocular disparity may help to solve the binocular matching problem.

When two arbitrary, uncorrelated images are projected to the two eyes, very little volumetric depth is experienced. We reasoned that, if a stimulus feature is involved in the matching of stimuli from the two eyes for depth perception, the range of perceived depth in complex stereoscopic displays will be greater when this feature is present than when it is absent (Fig. 1). To investigate the role of orientation, motion direction and speed in binocular matching, we generated a stimulus that allowed us to manipulate these stimulus dimensions independently. The stimulus consisted of an array of bars (Fig. 2a) uniformly distributed inside a three-dimensional volume. The bars were arranged in a series of frontoparallel planes, and their orientation, motion direction and speed were varied. Subjects judged the perceived depth-to-width ratio (Fig. 2b) of the volume of bars by adjusting the aspect ratio of an outline rectangle (Fig. 2c). In simple configurations containing only two oblique bars, very few false matches are possible, and the relative depth of the bars is readily recovered in both static and motion conditions. However, when many static bars with similar orientations are visible, more false matches are possible, and observers report a substantial reduction in their overall impression of depth. This reduction in depth presumably reflects a bias to match features that lie near the horopter, in other words those that have zero disparity. In principle, matching ambiguity could be considerably reduced if the visual system could use the motion direction, speed or orientation of the bars, or a combination of these features.

To investigate this possibility, we compared the perceived depth range of orientated bars that were presented either statically or with a gradient of motion (motion parallax). In the motion parallax condition, all of the bars moved simultaneously in the same direction and the speed of a bar decreased as the simulated distance from the observer increased. Perceived depth-to-width ratios for one subject are shown in Fig. 3a. These data show that: the perceived depth of the volume decreases as the number of bars increases; the fall-off in perceived depth is less when the range of orientations increases; and the perceived depth of the volume is greater with moving than with static bars.

The most interesting measure is the difference between the motion and the static conditions. Figure 3a (bottom row) and 3b shows this difference for one subject and the mean of the differences for three subjects, respectively. Note that each of the panels contains a local peak that shifts gradually to the right when the range of bar orientations increases. The perceived depth-to-width ratio as a function of orientation for an intermediate bar density (140 bars) is shown in Fig. 3c for the static display. The slope of the linear fit is significantly different from zero ($P < 0.003$, $r^2 = 0.91$), indicating that orientation, like motion, can disambiguate matching.

The results of experiment 1 revealed that both contour orienta-

tion and motion parallax enhance stereoscopically perceived depth. However, fixation was unrestricted, so it is not clear whether the benefit of motion arose from variations in speed, direction or both. We therefore tested four new motion conditions consisting of the possible permutations of the pairs (motion direction, speed) and (varying, static across bars). Fixation was restricted to dissociate the effects of direction and speed. To maximize our chances of observing significant differences, we used a bar density and orientation range that showed optimal depth facilitation of motion in experiment 1. Icons representing the bar motions are presented along the abscissa of the histogram in Fig. 4a for the six motion conditions. In the motion parallax condition (the leftmost panel), speed varied but motion direction was constant. The second condition resembled the motion parallax condition, but the depth of individual bars as specified by disparity was uncorrelated with the depth specified by motion parallax. Note that monocularly, the second condition is indistinguishable from the motion parallax condition, but binocularly, it generates a cue conflict. The conflict arises because bars with the same speed appear in a single depth plane when viewed monocularly, but appear in different depth planes when viewed binocularly (assuming that correct matches have been identified). In the third condition, bar motion was independent of the motion direction and the speed of neighbouring bars. The only constraint was that the same collection of speeds was used in this motion condition as in the first two conditions. In the fourth condition, the speed of individual bars was fixed (4.4° s^{-1}) but half of the bars moved to the right and the other half to the left. In the fifth motion condition, all the bars moved in the same direction with identical magnitudes. In this condition there was no differential motion. The rightmost icon represents the static condition.

The mean perceived depth-to-width ratios of experiment 2 are shown in Fig. 4a. Perceived depth in the static condition was much smaller than in the parallax condition, replicating the motion results of experiment 1. The critical data of this graph are depicted in the leftmost four panels, which show that the binocular conditions containing a range of speeds, motion directions or both are all effective in eliciting a percept of volumetric depth beyond that generated by either monocular motion or binocular disparity alone. These results show that speed, not just motion direction, can be used to disambiguate stereoscopic matches.

Our results contrast with a report that failed to find a benefit of speed in binocular matching⁷. To determine the cause of this difference, we attempted to replicate the results of that study using our method. We therefore constructed a random-dot display that contained only two motions and a small disparity difference between the two layers (4 arcmin). In this parameter regime, no significant differences in perceived depth were observed in the monocular and binocular displays containing only speed differences, but a large difference was observed for the display containing

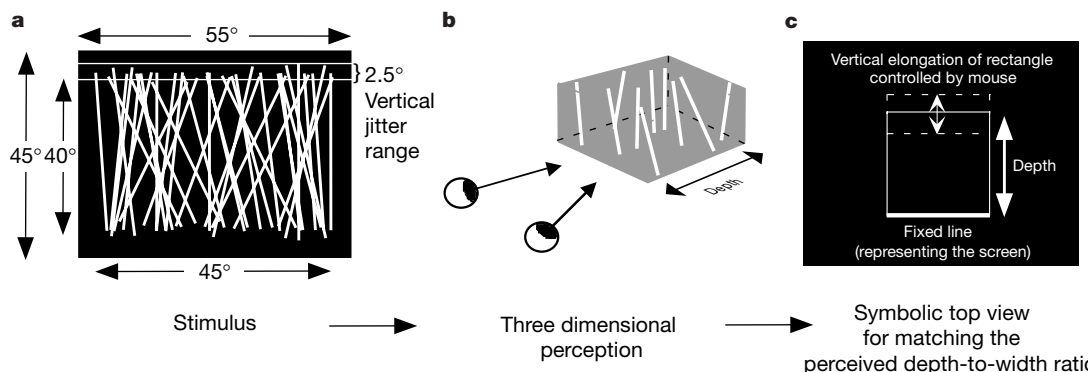


Figure 2 Experimental procedure. The stimulus consisted of a collection of frontoparallel bars (a) with disparities specifying a volume that evoked a percept of a three-dimensional

volume of bars (b). Observers matched the perceived depth-to-width ratio evoked by the stimulus with the aspect ratio of the outline rectangle (c).

different motion directions. However, the monocular percept of depth was much larger in the display containing only speed differences than in the display containing only direction differences. This suggests that the failure to obtain a benefit from speed in this parameter regime may be due to a Weber-law-like limitation on threshold sensitivity, wherein the ability to detect a just-noticeable difference scales with the standard against which it is compared. Indeed, when a suprathreshold disparity between the two layers of dots is introduced (30 arcmin), a clear benefit of speed is observed (Fig. 4c).

It is generally appreciated that disparity and motion parallax are powerful cues for the recovery of the volumetric aspects of a scene (for example, refs 10–13). It has been suggested that motion parallax and stereopsis generate independent depth estimates that are subsequently averaged to elicit an overall impression of depth¹⁴. Such a cue combination cannot account for our results. The perceived depth reported when motion and disparity were simultaneously present was larger than any weighted average of the depth elicited by these two cues when they were presented alone, even

when they were in conflict (second panel of Fig. 4a). This suggests that the primary role of motion, like orientation, is to provide information that can be used to establish binocular correspondence. This interpretation is also consistent with the phenomenological reports of observers. When little depth was experienced, the images took on the appearance of an uncorrelated stereogram, generating only a reduced impression of depth generated by the few spurious matches that formed near the horopter.

Since the work of Julesz¹⁵, one of the most fundamental and unresolved problems in stereoscopic research has concerned the primitives used to establish correspondence. Resolving this problem is critical for both computational theory and neurophysiological investigations into stereopsis. In contrast to earlier work that suggested that the matching primitives are unorientated⁸, our results support more recent findings that the mechanisms mediating human stereopsis are orientationally tuned⁹. In addition, our results show that both the direction and speed of moving targets can be used to resolve matching ambiguities. Many cells in V1 (ref. 2), MT (refs 3, 4) and MST (refs 5, 6) that are tuned to binocular

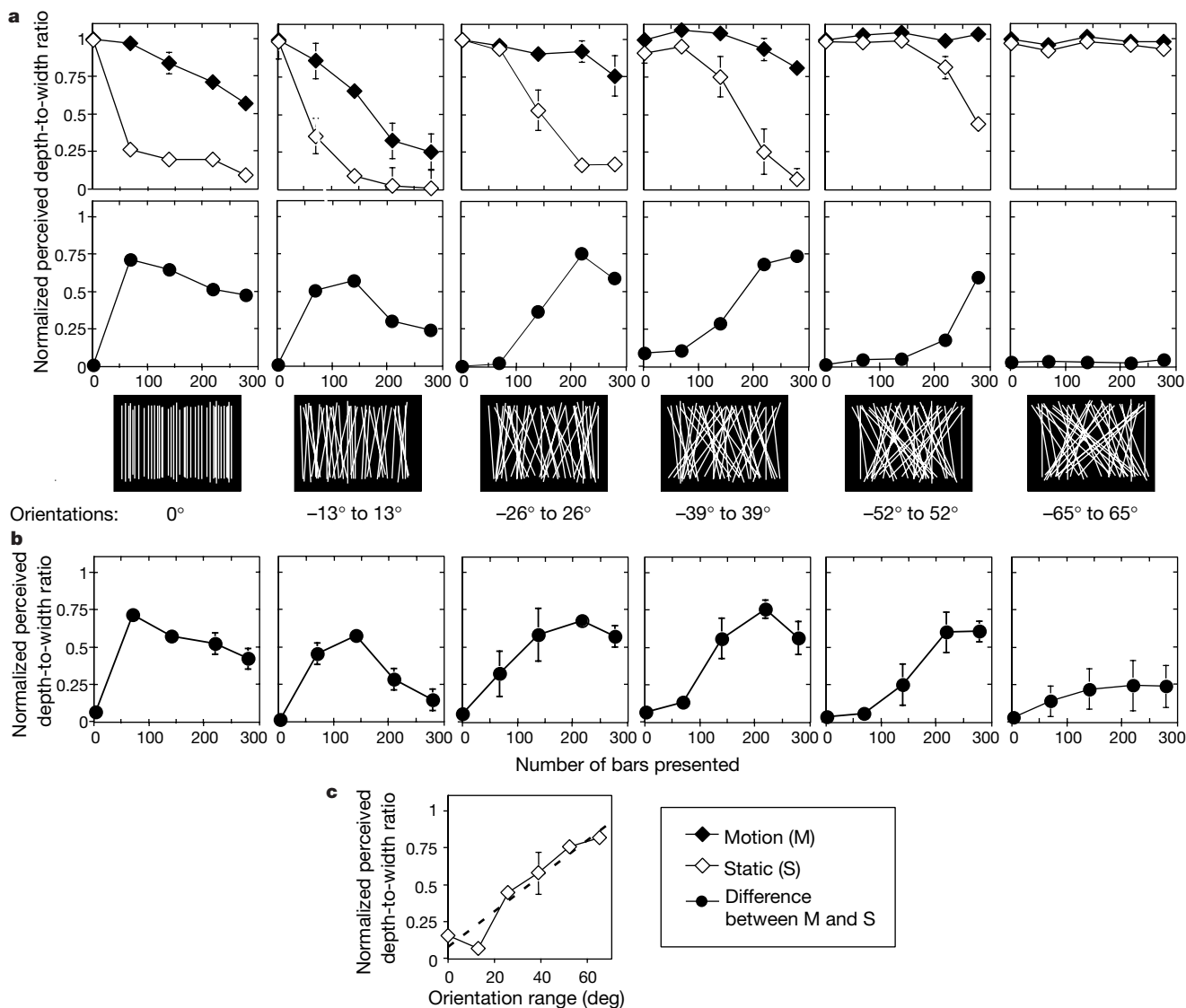


Figure 3 Results of experiment 1 showing the role of bar orientation and bar number. The icons in the centre depict the orientation range. **a**, Normalized perceived depth ratio as a function of the number of bars in the static and motion parallax conditions for observer J.E. (data from other observers are similar). The perceived depth ratio in the motion condition when only two bars were present was normalized to unity and all other depth

ratios were scaled by the same factor. Filled circles, differences in perceived depth ratio between the two conditions. **b**, Mean difference in perceived depth ratio between the static and motion parallax conditions across three subjects. Error bars, ± 1 s.d. **c**, Mean perceived depth-to-width ratio as a function of orientation for 140 static bars. Dashed line, a linear fit to the data ($r^2 = 0.91$).

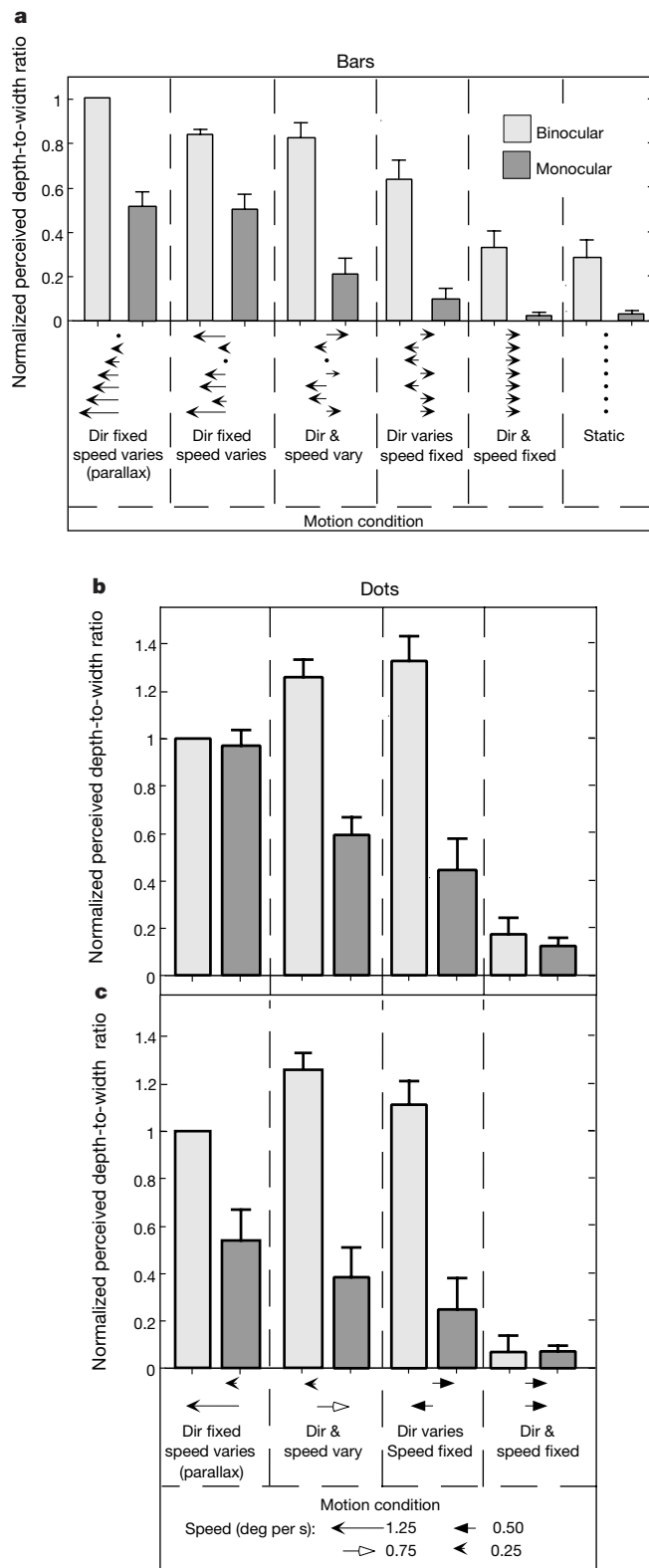


Figure 4 Results of experiments 2 and 3 showing the roles of motion direction and speed. The stimuli consisted of bars and dots, respectively. The motion conditions are depicted along the abscissa of the histograms. The perceived depth ratios in the motion parallax and stereo condition were normalized to unity and all other conditions were scaled accordingly. Dir, direction. **a**, Both speed and motion differences enhance perceived depth. **b**, Replication of ref. 7. For small disparity differences (4 arcmin), there is no clear benefit of speed. **c**, Replication of experiment 2. When the disparity difference between the two depth planes is sufficiently large (30 arcmin), a substantial benefit of speed is observed. Error bars, s.e. across three observers.

disparity are also tuned to orientation, motion direction and speed. Our results indicate that one of the functional roles of cells that multiplex motion information and orientation may be to facilitate binocular matching, shedding new light on the neural substrates that subservise stereopsis in primates.

Methods

The stimuli were anaglyph stereograms containing bright frontoparallel bars (10.8 arcmin widths) on a black background that were rear-projected onto a large flat screen. The displays were viewed from a distance of 2 m. The bars were presented behind the screen to avoid conflicting occlusion cues along the screen boundaries (note that any bar that intersected the left or right side of the display would monocularly appear to be occluded by the border of the screen). The far end of the volume had a relative disparity of 1.6°. The locations of bar end points were randomly chosen from a vertical range of 2.5° (independently of their orientation; Fig. 2a). The bars were randomly positioned within the volume such that the disparity steps between the bars was 1.6° divided by the number of bars. Overlap in the bars was possible due to the random positioning. The minimal and maximal values of disparity (0° and 1.6°) were present in all displays.

Subjects judged the perceived depth-to-width ratio of the volume by matching this to the aspect ratio of a rectangular display (Fig. 2c). Although the disparity range used was consistent with a volume that receded to 14 m, observers reported that the perceived depth was almost always smaller than the perceived width of the volume (and never exceeded the values available in the rectangular display). In each block of trials, all of the stimulus conditions appeared once in random order for 3.0 s. In each experiment there were ten trial blocks. In the motion conditions, the bars underwent a square-wave oscillation (left-right in a frontoparallel plane), reversing direction three times (two cycles). The bar speeds spanned the range of 1.2° s⁻¹ to 7.6° s⁻¹ (0.5 cycle was spanned by 20 frames). Observers R.E., R.F., J.E. and E.B. participated in experiment 1, and R.E., J.E. and E.B. participated in experiments 2 and 3.

Experiment 1

The stimuli subtended 45° horizontally by 40° vertically. The number of bars (2, 70, 140, 210 or 280) and their orientations varied across trials. Bar orientations were randomly chosen from a range of ±0, 13, 26, 39, 52 or 65°, centred about the vertical. The bars were presented either statically or with a gradient of motion, such that the speed decreased systematically with the depth specified by the bar's disparity (motion parallax). Eye movements were unrestricted. Each observer participated in 600 trials (5 numbers of bars, 6 bar orientation ranges, 2 motion conditions, 10 trial repetitions).

Experiment 2

We investigated static and motion parallax displays as well as four other motion conditions. These conditions consisted of the possible permutations of the pairs (direction, speed) and (varying, static across bars). Motion was again in the frontoparallel plane. Details about the motion conditions are provided in the main text. Viewing was either monocular or binocular. Observers were instructed to fixate a symbol to dissociate the effects of the direction and speed components of motion. The fixation symbol was an outline square (1.8° × 1.8°) with line segment widths of 5.4 arcmin. It was always presented in the plane of the screen (zero disparity). Under restricted fixation conditions, pilot work revealed that perceived depth was more vivid when a smaller stimulus size (20° × 20°) was used. We used a bar density and orientation that showed optimal facilitation of motion on perceived depth in experiment 1: there were 62 bars (the same density as resulted from 140 bars in experiment 1) and the orientation range was ± 26°. Thus, experiment 2 consisted of 120 trials (6 motion conditions, 2 viewing conditions, 10 trial repetitions).

Experiment 3

This experiment was identical to experiment 2, with the following modifications: 850 dots (5.4 × 5.4 arcmin²) were used instead of bars; only two layers were simulated; and the display size was reduced to 8° × 5°. The parametric changes were introduced to simulate more closely the conditions studied in ref. 7. The nearest layer had zero disparity. The more distant layer had a disparity of 4 arcmin in the first session and 30 arcmin in the second. The motion direction and speed were uniform within each layer. The permutations of the pairs (motion direction, speed) and (varying, static) were tested. Dot speeds (0.25, 0.50, 0.75 or 1.25° s⁻¹) were chosen such that the differential speed between the two layers was 1° s⁻¹.

Received 16 August 2000; accepted 14 January 2001.

- Howard, I. P. & Rogers, B. J. *Binocular Vision and Stereopsis* (Oxford Univ. Press, New York, 1995).
- Poggio, G. F. & Talbot, W. H. Mechanisms of static and dynamic stereopsis in foveal cortex of the rhesus monkey. *J. Physiol.* **315**, 469–492 (1981).
- Bradley, D. C., Qian, N. & Andersen, R. A. Integration of motion and stereopsis in middle temporal cortical area of macaques. *Nature* **373**, 609–611 (1995).
- Maunsell, J. H. & Van Essen, D. C. Functional properties of neurons in middle temporal visual area of the macaque monkey. II. Binocular interactions and sensitivity to binocular disparity. *J. Neurophysiol.* **49**, 1148–1167 (1983).
- Roy, J. P. & Wurtz, R. H. The role of disparity-sensitive cortical neurons in signalling the direction of self-motion. *Nature* **348**, 160–162 (1990).
- Roy, J. P., Komatsu, H. & Wurtz, R. H. Disparity sensitivity of neurons in monkey extrastriate area MST. *J. Neurosci.* **12**, 2478–2492 (1992).

- Bradshaw, M. F. & Cumming, B. G. The direction of retinal motion facilitates binocular stereopsis. *Proc. R. Soc. Lond. B* **264**, 1421–1427 (1997).
- Mayhew, J. E. & Frisby, J. P. Stereopsis masking in humans is not orientationally tuned. *Perception* **7**, 431–436 (1978).
- Mansfield, J. S. & Parker, A. J. An orientation-tuned component in the contrast masking of stereopsis. *Vision Res.* **33**, 1535–1544 (1993).
- Rogers, B. J. & Graham, M. E. Similarities between motion parallax and stereopsis in human depth perception. *Vision Res.* **22**, 261–270 (1982).
- Bradshaw, M. F. & Rogers, B. J. The interaction of binocular disparity and motion parallax in the computation of depth. *Vision Res.* **36**, 3457–3468 (1996).
- Tittle, J. S. & Braunstein, M. L. Recovery of 3-D shape from binocular disparity and structure from motion. *Percept. Psychophys.* **54**, 157–169 (1993).
- Richards, W. Structure from stereo and motion. *J. Opt. Soc. Am. A* **2**, 343–349 (1985).
- Landy, M. S., Maloney, L. T., Johnston, E. B. & Young, M. Measurement and modeling of depth cue combination: in defense of weak fusion. *Vision Res.* **35**, 389–412 (1995).
- Julesz, B. *Foundations of Cyclopean Perception* (Univ. Chicago Press, Chicago, 1971).

Acknowledgements

R.v.E. was supported by a NIH grant awarded to B.A. and by the Royal Netherlands Academy of Arts and Sciences, and B.A. was supported in part by NIH.

Correspondence and requests for materials should be addressed to B.L.A. (e-mail: bart@mit.edu).

The homeobox gene *lim-6* is required for distinct chemosensory representations in *C. elegans*

Jonathan T. Pierce-Shimomura, Serge Faumont, Michelle R. Gaston, Bret J. Pearson & Shawn R. Lockery

Institute of Neuroscience, 1254 University of Oregon, Eugene, Oregon 97403, USA

The ability to discriminate between different chemical stimuli is crucial for food detection, spatial orientation and other adaptive behaviours in animals. In the nematode *Caenorhabditis elegans*, spatial orientation in gradients of soluble chemoattractants (chemotaxis) is controlled mainly by a single pair of chemosensory neurons¹. These two neurons, ASEL and ASER, are left–right homologues in terms of the disposition of their somata and processes, morphology of specialized sensory endings, synaptic partners and expression profile of many genes^{2,3}. However, recent gene-expression studies have revealed unexpected asymmetries between ASEL and ASER. ASEL expresses the putative receptor guanylyl cyclase genes *gcy-6* and *gcy-7*, whereas ASER expresses *gcy-5* (ref. 4). In addition, only ASEL expresses the homeobox gene *lim-6*, an orthologue of the human *LMX1* subfamily of homeobox genes⁵. Here we show, using laser ablation of neurons and whole-cell patch-clamp electrophysiology, that the asymmetries between ASEL and ASER extend to the functional level. ASEL is primarily sensitive to sodium, whereas ASER is primarily sensitive to chloride and potassium. Furthermore, we find that *lim-6* is required for this functional asymmetry and for the ability to distinguish sodium from chloride. Thus, a homeobox gene increases the representational capacity of the nervous system by establishing asymmetric functions in a bilaterally symmetrical neuron pair.

To determine whether *C. elegans* can distinguish between the attractants sodium and chloride in our experimental system⁶, we performed a discrimination test in which we examined the chemotaxis performance of worms in a gradient of sodium (50 μM to 10 mM) superimposed on a saturating background concentration of chloride (100 mM), and vice versa (Fig. 1a, d). In both cases, worms migrated toward the peak of the gradient as expected⁷,

although the overall chemotaxis performance was reduced relative to control worms tested in sodium or chloride gradients but with no background ion concentration (Fig. 1b, d).

However, the chemotaxis performance of worms tested under conditions in which the gradient and background concentration contained the same ion (Fig. 1c, d) degenerated to roughly chance level, defined as the chemotaxis performance of worms tested in the absence of a gradient (Fig. 1d, dotted line). Together, these results show that sodium chemotaxis persists against a background of

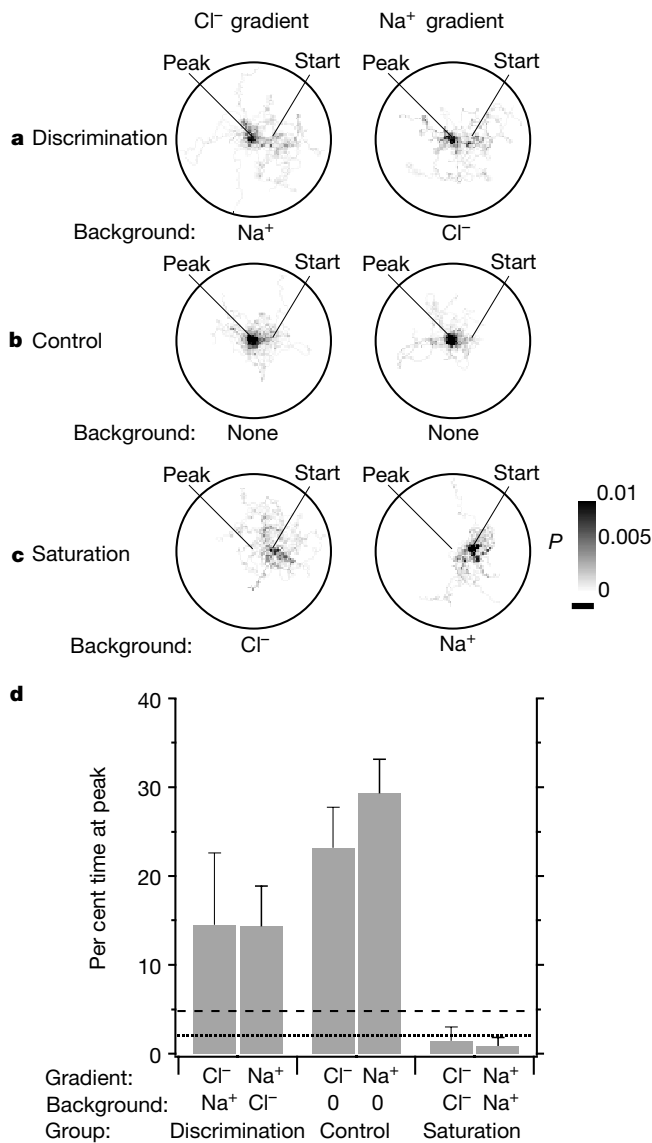


Figure 1 Discrimination of sodium and chloride by wild-type *C. elegans*. **a–c**, Probability density plots for worms assayed in gradients of chloride (left) and sodium (right) originating at the centre of the plate (peak), *n* ≥ 15. Grey scale indicates the probability per unit area of finding a worm at a given location in the plate during the 20-min assay. Scale bar, 1 cm. **a**, Discrimination. Worms located and remained at the peak of a chloride gradient superimposed on a high background concentration (100 mM) of sodium, or at the peak of a sodium gradient superimposed on a high background concentration (100 mM) of chloride. **b**, Control. Chemotaxis performance was normal in gradients identical to those in **a** when the background ion was omitted. **c**, Saturation. Worms failed to locate the peak of the gradient when it was superimposed on a high background concentration (100 mM) of the same ion. **d**, Average per cent time spent at the gradient peak for worms in the six conditions shown in **a–c**. Dotted line indicates mean chance performance, measured by assaying 74 worms in plates with neither gradient nor background. Dashed line indicates upper 95 per cent confidence limit for mean chance performance.